



Adsorption of Co(II) and Mn(II) ions from pure terephthalic acid wastewater onto Na-bentonite

Changshen Ye, Meihong Lin, Zhaoyang Qi, Wenjie Zhu, Chen Yang, Ting Qiu*

School of Chemical Engineering, Fuzhou University, Fuzhou 350116, China, emails: fzycsyrfyq@fzu.edu.cn (C. Ye), 573438303@qq.com (M. Lin), 1028857587@qq.com (Z. Qi), 1060949770@qq.com (W. Zhu), cyang@fzu.edu.cn (C. Yang), Tel. +86 13705945511; email: tingqiu@fzu.edu.cn (T. Qiu)

Received 12 May 2015; Accepted 14 October 2015

ABSTRACT

Removal of Co(II) and Mn(II) ions from the pure terephthalic acid (PTA) wastewater onto Na-bentonite has been investigated in this work. Batch experiments were performed to elucidate the effects of various parameters, such as dosage of adsorbent, temperature, and initial pH, on the adsorption process. It has been found that the simulated adsorption process of the pseudo-second-order kinetic model was in better agreement with experimental results than that of the pseudo-first-order and intra-particle diffusion kinetic models. Moreover, the adsorption experiments were conducted at four temperatures, which was 298.15, 308.15, 318.15, and 328.15 K, respectively, with the initial metal concentrations ranging from 30 to 120 mg L⁻¹, so as to study the adsorption thermodynamics. Compared with the Freundlich and Dubinin–Radushkevich models, the Langmuir isotherm model agreed better with experimental data. The Gibb's free energy change (ΔG), enthalpy change (ΔH), and entropy change (ΔS) of the adsorption process were calculated at four temperatures. The results indicated that the adsorption process was endothermic and spontaneous. When the adsorbent concentration was 3 g L⁻¹, the adsorption percentages of Co(II) and Mn(II) can be attained about 95.09 and 95.03%, respectively. Therefore, it can be concluded that Na-bentonite could be used as an efficient adsorbent to remove heavy metal ions from the PTA wastewater.

Keywords: Co(II) and Mn(II) ions; Adsorption; Na-bentonite; Adsorption isotherm; Adsorption mechanism

1. Introduction

As reported, the amount of effluent produced in the refined unit of the pure terephthalic acid (PTA) has surpassed 18 million tons in 2005 in China [1]. In 2015, the PTA wastewater will reach to 70 million tons. In the wastewater, there are some high-concentration components, such as p-toluylic acid and

p-xylene, and heavy metal pollutants, such as Co(II) and Mn(II) ions, which are worthy of more than 2000 million RMB. Co(II) and Mn(II) ions used as catalysts in PTA industry are difficult to be removed completely due to their low concentrations in solutions. In order to recycle the precious metal ions and protect the environment, Co(II) and Mn(II) ions must be eliminated from effluents discharged from factories.

*Corresponding author.

The removal of heavy metal pollutants at low concentration from aqueous solution could not be easy by conventional ways. It has been proved that such contaminants were more effectively removed by ion exchange or adsorption onto solid adsorbents such as activated carbon [2] or bentonite materials. Many inorganic metals, for instance, Cu(II), Pb(II), Zn(II), Cd(II), and Co(II), adsorbed from wastewater by bentonite have already been reported in the previous literatures [3–5]. Kubilay et al. [3] studied the removal of Cu(II), Zn(II), and Co(II) ions from aqueous solution by natural bentonite and pointed out that bentonitic clay holds great potential to remove the relevant heavy metal cations from industry wastewater. Gözen et al. [4] investigated the adsorption of Pb(II), Cd(II), Cu(II), and Zn(II) from aqueous solutions onto Bentonite. The results indicated that bentonite was a good adsorbent for Zn(II), Cd(II), Pb(II), and Cu(II) without the need for any chemical treatment by comparison with the treated clay [5].

Bentonite is known as an excellent adsorbent due to its large specific area, cation exchange capacity, and adsorptive affinity for inorganic ions. In addition, it is readily available, cheap, and environment friendly. Bentonite is mainly composed of montmorillonite, which is a 2:1-type aluminosilicate, namely two silica tetrahedral sheets with a central aluminum octahedral. The isomorphous substitution of Al^{3+} for Si^{4+} in the tetrahedral layer and Mg^{2+} for Al^{3+} in the octahedral layer leads to a net negative charge on the bentonite surface. This charge imbalance is offset by exchangeable cations (Na^+ and Ca^{2+} , etc.) at the layer surfaces [6], giving clay the ability to attract and hold cations such as toxic heavy metals through ion exchange. In general, the ion-exchange capacity of Na-bentonite is superior to calcium base bentonite, so Na-bentonite was selected as the adsorbent for Co(II) and Mn(II).

2. Experimental procedures

2.1. Materials and characterization

Na-bentonite used in the experiments was purchased from Jinfeng Jingshui Company of Henan province, China. Bentonite was washed with deionized water and edulcorated and then sieved through a 75- μm sieve. Note that it should be dried at 393.15 K in an electric oven for 120 min prior to use. The main chemical compositions of Na-bentonite are given in Table 1. The main properties of Na-bentonite are shown in Table 2. Co(II) and Mn(II) ions solutions were prepared by dissolving $\text{Co}(\text{CH}_3\text{COO})_2 \cdot 4\text{H}_2\text{O}$ and $\text{Mn}(\text{CH}_3\text{COO})_2 \cdot 4\text{H}_2\text{O}$ in deionized water. All chemicals used in this work were of analytical purity and

Table 1

Chemical analysis results of Na-bentonite (percent mass content)

Sample	Percent mass content
SiO_2	65.20
Al_2O_3	17.25
Fe_2O_3	3.10
MgO	3.10
CaO	1.2
K_2O	0.86
Na_2O	4.15

Table 2

Properties of Na-bentonite

Property	Na-bentonite
BET surface area ($\text{m}^2 \text{g}^{-1}$)	31.9875
Total pore volume (mL g^{-1})	0.0808
Pore size (nm)	10.102
Particle size (mm)	0.60–0.75

purchased from Aldrich Chemical Co. and Sinopharm Chemical Reagent Co. Ltd., China. Hence, all chemicals were used without the further purification. Initial pH of the aqueous solutions was adjusted by 0.1 mol L^{-1} NaOH and HCl solutions.

Surface morphology of the adsorbent was observed by scanning electron microscopy (SEM, Hitachi Ltd., S-4800). The specific surface area and pore size of the adsorbent were determined by Brunauer–Emmett–Teller (BET) method with 3 Flex (Micrometric Ltd, USA). X-ray diffraction analysis of the adsorbent was carried out by Miniflex II X-ray diffractometer (XRD) equipment from Rigaku Corporation.

2.2. Batch adsorption studies

The adsorption of heavy metals onto Na-bentonite was carried out using the batch technique. A certain amount of bentonite was placed in 250-mL conical flasks containing 100 mL of Co(II) or Mn(II) ions solution of known concentrations. Then, the flask was shaken at 200 rpm in a thermostat for a desired time. Initial pH and temperatures of aqueous solutions were also taken into consideration. Subsequently, the solutions were centrifuged for 10 min at 4,000 rpm in a centrifuge and the residual metal concentrations in aqueous solution were measured by inductively coupled plasma (ICPE-9000, Shimadzu Corporation).

2.3. Data procession

The adsorption percentage and the adsorption capacity were calculated from the following equations, respectively:

$$\eta = \frac{C_0 - C_e}{C_0} \times 100\% \quad (1)$$

$$Q_e = \frac{(C_0 - C_e)}{m} \times V \quad (2)$$

where η (%) is the adsorption percentage, Q_e (mg g^{-1}) is the amount of adsorbed metal ion per unit adsorbent mass at equilibrium, C_0 (mg L^{-1}) is the initial concentration of the metal solution, C_e (mg L^{-1}) is the equilibrium concentration of the solution, m (g) and V (mL) are the mass of bentonite and the volume of the aqueous solution, respectively. All experimental data were performed in triplicate and the relative errors of the data were less than 5%.

3. Results and discussion

3.1. Effect of contact time

The adsorption of Co(II) and Mn(II) ions onto bentonite was studied as a function of contact time from 2 min to 60 min at 298.15 K with a constant initial ion concentration of 30 mg L^{-1} . Fig. 1 showed that the adsorption percentage varies with the contacting time.

As can be seen from Fig. 1, both Co(II) and Mn(II) were rapidly adsorbed onto bentonite and then

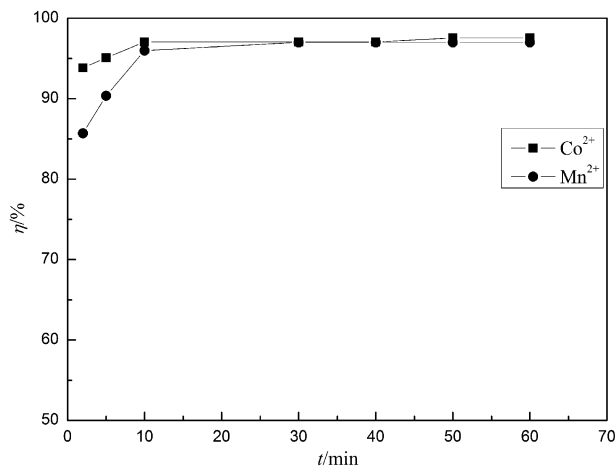


Fig. 1. Effect of contacting time on the adsorption of metal ions on Na-bentonite ($C_{\text{Co}^{2+}} = 30 \text{ mg L}^{-1}$; $C_{\text{Mn}^{2+}} = 30 \text{ mg L}^{-1}$; $C_m = 3 \text{ g L}^{-1}$; $r = 200 \text{ rpm}$; $T = 298.15 \text{ K}$; $\text{pH} = 7$; $V = 100 \text{ mL}$).

approached to an equilibrium level within 10 min. Therefore, 60-min contacting time was found to be long enough for maximum adsorption and can be used in subsequent experiments. The fast adsorption of these two heavy metal ions onto Na-bentonite showed that the uptake of heavy metal ions from solution to bentonite was mainly dominated by chemical adsorption rather than physical adsorption. Similarly, the uptake of Cd(II) by GMZ bentonite achieved adsorption equilibrium quickly [7].

3.2. Effect of initial pH

The effect of initial pH on the adsorption of Co(II) and Mn(II) ions onto bentonite was investigated by varying the initial pH of the metal aqueous solution-bentonite suspension from 1.5 to 9 at 298.15 K, and keeping the metal ions concentrations of 30 mg L^{-1} . As shown in Fig. 2, it can be found that the adsorption percentages of metal ions increased with initial pH of the solution in the range of 1.0–6.0. However, the adsorption percentage reached a plateau and was no more enhanced as the initial pH above 6. The same results have been presented in other studies [6,8,9].

The changes of H^+ and OH^- ions in solution will cause the surface functional groups and clay minerals to protonate and deprotonate by adsorption of H^+ or OH^- ions, respectively, as shown in following Eqs. (3) and (4) [3]:

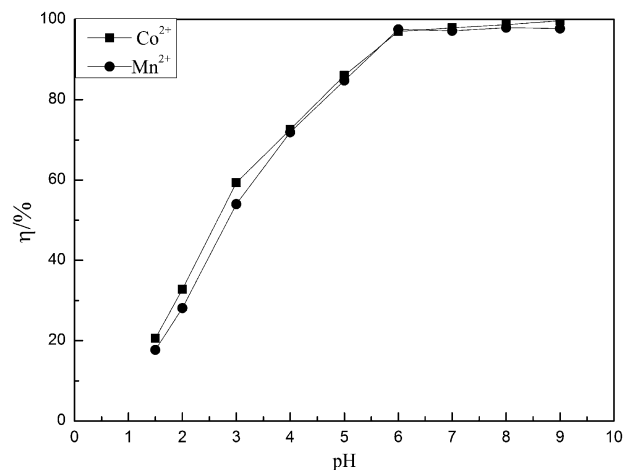
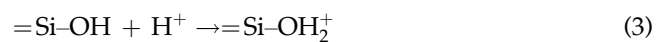
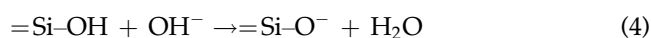


Fig. 2. Effect of initial pH on the adsorption of metal ions on Na-bentonite ($C_{\text{Co}^{2+}} = 30 \text{ mg L}^{-1}$; $C_{\text{Mn}^{2+}} = 30 \text{ mg L}^{-1}$; $C_m = 3 \text{ g L}^{-1}$; $r = 200 \text{ rpm}$; $T = 298.15 \text{ K}$; $t = 60 \text{ min}$; $V = 100 \text{ mL}$).



Therefore, the metal ions will compete with H^+ for the available adsorption sites at low pH condition, leading to the less adsorption percentage. The negative charges increased with the rise of initial pH in the solutions according to Eq. (4). Consequently, the contribution of ion competition will decrease with a further increase in initial pH, and the adsorption percentage will increase too. As the initial pH is beyond 6, the adsorption percentage has attained a maximum value. At higher initial pH, the adsorption percentage increased slightly, for which some precipitation was developed. Given the above analysis, in the further experiments pH 7 was selected. Under this condition, the main mechanism of adsorption is ion exchange.

3.3. Effect of adsorbent dosage

The effect of adsorbent dosage on adsorption of Co(II) and Mn(II) ions onto bentonite was explored at 298.15 K by varying the adsorbent amount from 0.02 to 0.8 g. As presented in Fig. 3, it can be clearly seen that the adsorption percentage increased with the rise of adsorbent dosage. When the adsorbent concentration came to 3 g L^{-1} , the adsorption percentages approached to 95.09% for Co(II) and 95.03% for Mn(II), respectively. The results were due to the greater availability of the exchangeable/adsorption sites at the higher concentration of the adsorbent. With the

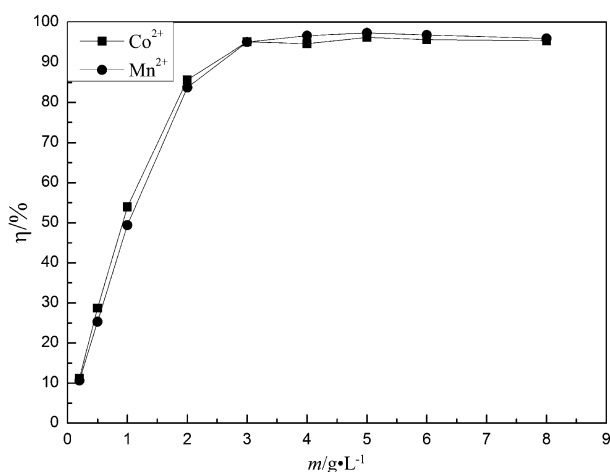


Fig. 3. Effect of adsorbent dosage on the adsorption of metal ions on Na-bentonite ($C_{Co^{2+}} = 30 \text{ mg L}^{-1}$; $C_{Mn^{2+}} = 30 \text{ mg L}^{-1}$; $t = 60 \text{ min}$; $r = 200 \text{ rpm}$; $T = 298.15 \text{ K}$; $\text{pH} = 7$; $V = 100 \text{ mL}$).

further increase of adsorbent concentration, there was no higher adsorption efficiency, for which the metal ions in aqueous solution and on the adsorbent have arrived to a mutual equilibrium state. These results also suggested that the higher bentonite content was not necessary in order to achieve a high adsorption yield. On the basis of these results, 3 g L^{-1} of the bentonite was used for subsequent studies.

3.4. Effect of temperature

The effect of temperature on the adsorption of Co(II) and Mn(II) ions onto bentonite was discussed with the solutions temperature varied at 298.15, 308.15, 318.15, and 328.15 K. It has been found from Fig. 4 that the adsorption percentages of Co(II) and Mn(II) increased from 95.08 to 97.01% and from 95.70 to 97.57%, respectively, as the temperature increased from 298.15 to 328.15 K. Therefore, high temperature is helpful for the adsorption of Co(II) and Mn(II).

3.5. Adsorption kinetics

The pseudo-first-order model, pseudo-second-order kinetic model, and the intraparticle diffusion model were used to study the adsorption kinetics of Co(II) and Mn(II) ions.

The pseudo-first-order kinetic model has the following linear form [10]:

$$\ln(Q_c - Q_t) = \ln Q_c - k_1 t \quad (5)$$

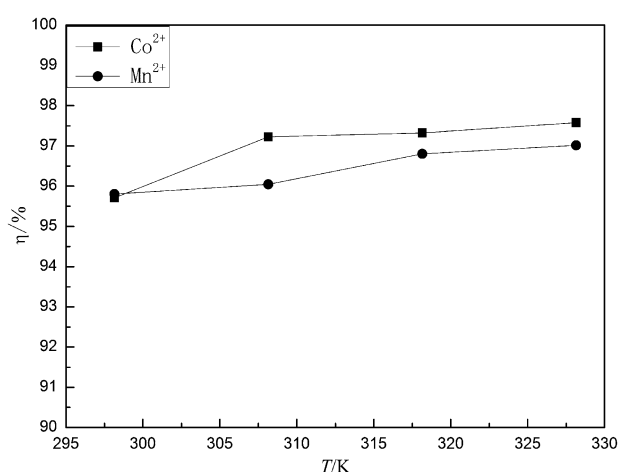


Fig. 4. Effect of temperature on the adsorption of metal ions on Na-bentonite ($C_{Co^{2+}} = 30 \text{ mg L}^{-1}$; $C_{Mn^{2+}} = 30 \text{ mg L}^{-1}$; $C_m = 3 \text{ g L}^{-1}$; $r = 200 \text{ rpm}$; $t = 60 \text{ min}$; $\text{pH} = 7$; $V = 100 \text{ mL}$).

The pseudo-second-order kinetic model has the general expression [11]:

$$\frac{t}{Q_t} = \frac{1}{k_2 Q_e^2} + \frac{t}{Q_e} \quad (6)$$

where Q_t (mg g^{-1}) is the amount of metal ion adsorbed on the adsorbent at time t (min), k_1 (min^{-1}) and k_2 ($\text{g mg}^{-1} \text{min}^{-1}$) are the rate constants for the pseudo-first-order and pseudo-second order kinetic models, respectively.

The equation on the intraparticle diffusion model is [12]:

$$Q_t = k_3 t^{1/2} + C \quad (7)$$

where k_3 ($\text{mg g}^{-1} \text{min}^{-1/2}$) is the intraparticle diffusion rate constant and C (mg g^{-1}) is a constant.

The adsorption kinetics were studied using 100 mL 30 mg L^{-1} of Co(II) and Mn(II) ions under the conditions of pH 7, $C_m = 3 \text{ g L}^{-1}$, $r = 200 \text{ rpm}$, and $T = 298.15 \text{ K}$. The contacting time varied from 2 to 60 min. The experiments were conducted by batch method, and the remaining concentrations of metals were measured at regular intervals during the process by taking out one conical flask.

Experimental data were analyzed using the pseudo-first-order, pseudo-second-order kinetics, and the intraparticle diffusion models. The kinetic parameters at 298.15 K of the three models were tabulated in Table 3. The pseudo-first-order and intraparticle diffusion models cannot describe the adsorption process of Co(II) and Mn(II) ions onto bentonite well since the correlation coefficients (R^2) were low. However, the correlation coefficients for the pseudo-second-order kinetic model were higher than those of the pseudo-first-order and the intraparticle diffusion models. Thus, the adsorption of Co(II) and Mn(II) ions on Na-bentonite followed the pseudo-second-order rate expression, and the calculated equilibrium adsorption capacity matched with the actual equilibrium adsorption capacity well. This implied that the removal of

Co(II) and Mn(II) ions belonged to chemical adsorption rather than physical adsorption process [13].

3.6. Adsorption isotherms

The Langmuir, Freundlich, and Dubinin–Radushkevich (D–R) isotherms are the most widely used isothermal adsorption equations to describe the adsorption behaviors of heavy metals in aqueous solutions.

3.6.1. The Langmuir isotherm

The Langmuir model is usually used to describe the monomolecular layer adsorption. The basic assumption is that the adsorption behavior only occurred on the specific and uniform adsorption sites; there is no interaction between the adsorbate molecules [14–16]. The Langmuir isothermal adsorption equation is:

$$\frac{C_e}{Q_e} = \frac{1}{Q_m K_L} + \frac{C_e}{Q_m} \quad (8)$$

where K_L (L mg^{-1}) and Q_m (mg g^{-1}) are Langmuir equilibrium constants related to adsorption energy and adsorption capacity, respectively; C_e (mg g^{-1}) is the equilibrium concentration of metal in solution, while Q_e (mg g^{-1}) is the amount of metal ions adsorbed onto adsorbent in equilibrium. The equilibrium data are shown in Fig. 5 for Co(II) and Fig. 6 for Mn(II). The Langmuir model parameters and the statistical fits are provided in Table 4.

3.6.2. The Freundlich isotherm

The Freundlich model is an empirical equation used to describe the nonideal adsorption. Hence, this model cannot forecast the saturated adsorption capacity. However, it can describe not only the single layer adsorption, but also multilayer adsorption [17–19]. When the adsorbate concentration is proper in

Table 3
Kinetics model parameters of adsorption of heavy metal ions onto Na-bentonite at 298.15 K

Metal	Pseudo-first-order model			Pseudo-second-order model			Intraparticle diffusion model			
	Q_{1e} (mg g^{-1})	k_1 (min^{-1})	R^2	Q_{2e} (mg g^{-1})	k_2 ($\text{g mg}^{-1} \text{min}^{-1}$)	R^2	k_3 ($\text{mg g}^{-1} \text{min}^{-1/2}$)	C	R^2	Q_e (mg g^{-1})
Co ²⁺	6.0000	0.0445	0.553	5.9844	17.4515	1.000	0.0140	5.8688	0.580	5.4541
Mn ²⁺	5.3800	0.0644	0.832	5.3792	95.9900	1.000	0.0489	4.9692	0.668	5.5103

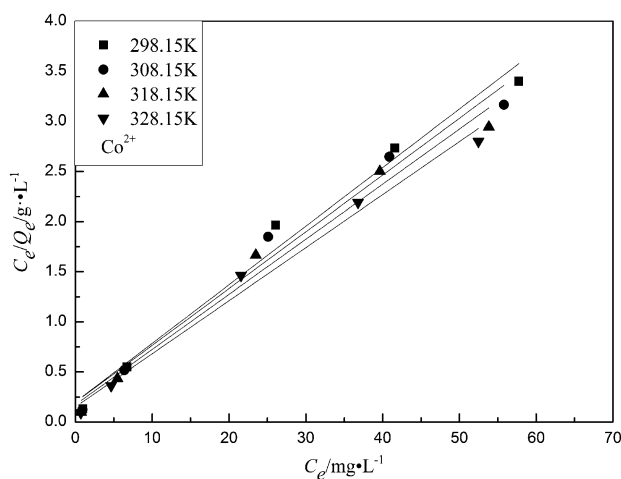


Fig. 5. Langmuir adsorption isotherm of Co(II) ion on Na-bentonite. ($C_m = 3 \text{ g L}^{-1}$; $r = 200 \text{ rpm}$; $\text{pH} = 7$; $V = 100 \text{ mL}$; $t = 60 \text{ min}$).

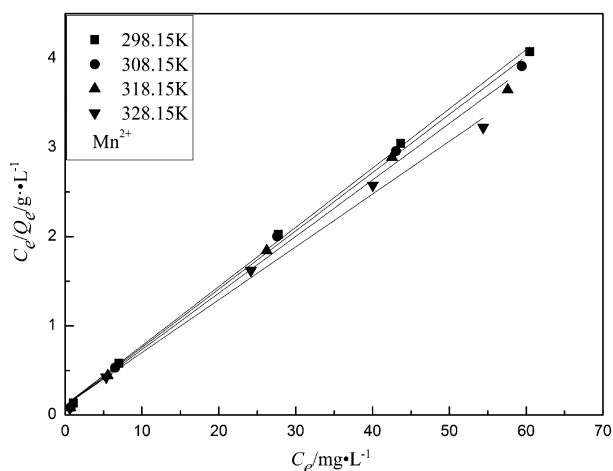


Fig. 6. Langmuir adsorption isotherm of Mn(II) ion on Na-bentonite. ($C_m = 3 \text{ g L}^{-1}$; $r = 200 \text{ rpm}$; $\text{pH} = 7$; $V = 100 \text{ mL}$; $t = 60 \text{ min}$).

aqueous solution, the adsorption equilibrium data always fitted the Langmuir and Freundlich models at the same time. It is monomolecular layer adsorption when the adsorbate concentration is low, while it is likely multilayer adsorption when the adsorbate concentration is high.

The Freundlich isothermal adsorption equation may be written as follows:

$$\ln Q_e = \frac{1}{n} \ln C_e + \ln K_F \quad (9)$$

where K_F (mg g^{-1}) and n are the Freundlich constants and adsorption intensity, respectively. According to

the Freundlich theory, n can be used to determine whether the adsorption is favorable or not. When $n > 1$, it is favorable adsorption; when $n = 1$, it is linear adsorption; when $n < 1$, it is unfavorable adsorption [20].

The results are presented in Fig. 7 for Co(II) and Fig. 8 for Mn(II); the Freundlich model parameters and the statistical fits are given in Table 4.

3.6.3. The D–R isotherm

The D–R model can be used to judge whether the adsorption is physical or chemical adsorption (Figs. 9 and 10). E (kJ mol^{-1}) is often used to judge the adsorption type in the D–R model. The value of mean adsorption energy $E < 8.00$ and $E > 8 \text{ kJ mol}^{-1}$ belongs to physical and chemical adsorption, respectively [21].

The isothermal adsorption equation [22] is:

$$\ln q_e = \ln q_m - \beta \varepsilon^2 \quad (10)$$

where q_e (mol g^{-1}) is the amount of metal ions adsorbed onto per unit weight of adsorbent in equilibrium, Q_m (mol g^{-1}) is the maximum adsorption capacity, β ($\text{mol}^2 \text{J}^{-2}$) is the capacity coefficient related to mean adsorption energy, and ε is the Polanyi potential, which is equal to:

$$\varepsilon = RT \left(1 + \frac{1}{C_{e1}} \right) \quad (11)$$

where R ($\text{J mol}^{-1} \text{K}^{-1}$) is the gas constant and T (K) is the temperature. C_{e1} (mol L^{-1}) is the equilibrium concentration of metal in solution. The saturation limit, Q_{mv} , may represent the total specific micropores volume of the adsorbent. The adsorption potential is independent of the temperature but varies according to the nature of adsorbent and adsorbate. The slope of the plot of $\ln q_e$ against ε^2 gives β and the intercept, and then the adsorption capacity was obtained. The adsorption space in the vicinity of a solid surface is characterized by a series of equipotential surfaces having the same adsorption potential. This adsorption potential is independent of the temperature but varies according to the nature of adsorbent and adsorbate. The adsorption energy E might be given by the following relationship:

$$E = \frac{1}{\sqrt{2\beta}} \times 10^3 \quad (12)$$

The plot of $\ln q_e$ vs. ε^2 for metal ions adsorption onto Na-bentonite was drawn with the statistic of linear

Table 4

Langmuir, Freundlich, and D–R parameters of adsorption isotherm of heavy metals on Na-bentonite at different temperatures

Metal	T (K)	Langmuir			Pseudo-second-order model			D–R			
		Q_m (mg g ⁻¹)	K_L (L g ⁻¹)	R^2	K_F (mg g ⁻¹)	n	R^2	$\beta \times 10^8$ (mol ² kJ ⁻²)	Q_m (mg g ⁻¹)	E (kJ mol ⁻¹)	R^2
Co (II)	298.15	17.0940	0.2928	0.980	2.4390	5.4142	0.942	0.1677	26.5919	17.2671	0.951
	308.15	17.6429	0.2868	0.976	2.4520	5.2687	0.945	0.1604	24.9758	17.6556	0.952
	318.15	18.1818	0.3170	0.976	2.5080	5.3419	0.944	0.1466	28.4545	18.4679	0.953
	328.18	18.8679	0.3524	0.984	2.5398	5.1493	0.950	0.1425	30.5849	18.7317	0.964
Mn (II)	298.15	15.0602	0.5858	0.999	2.4942	6.5656	0.944	0.1414	22.6545	18.8044	0.970
	308.15	15.3116	0.6169	0.997	2.5648	7.1870	0.965	0.1174	21.8251	20.6372	0.985
	318.15	15.7828	0.6276	0.996	2.5695	6.9881	0.944	0.1133	22.8594	21.0073	0.968
	328.15	16.8862	0.5448	0.994	2.6002	6.3702	0.972	0.1153	25.1073	20.8243	0.988

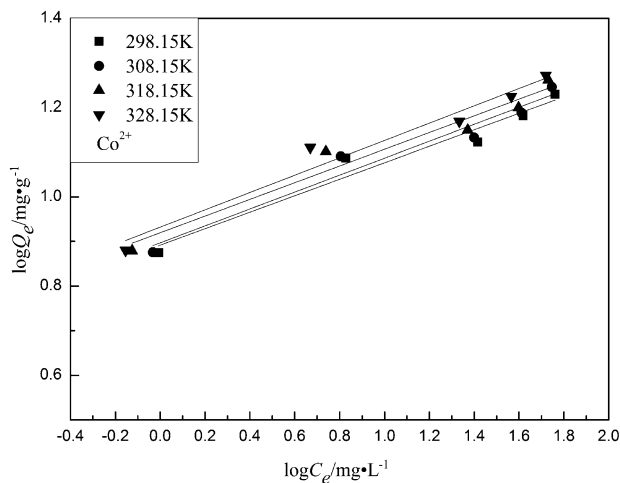


Fig. 7. Freundlich adsorption isotherm of Co(II) ion on Na-bentonite. ($C_m = 3 \text{ g L}^{-1}$; $r = 200 \text{ rpm}$; $\text{pH} = 7$; $V = 100 \text{ mL}$; $t = 60 \text{ min}$).

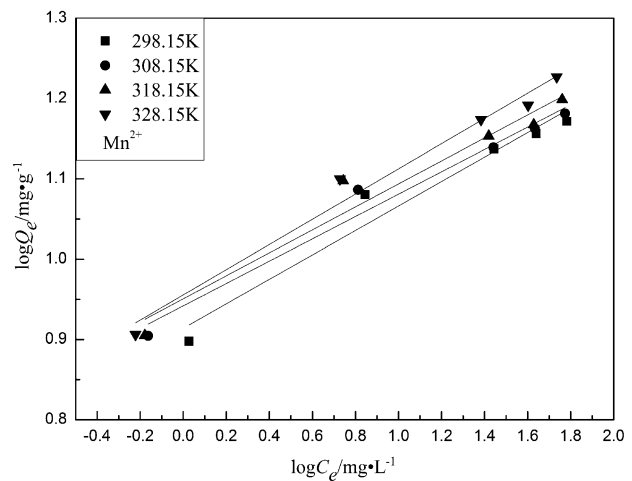


Fig. 8. Freundlich adsorption isotherm of Mn(II) ion on Na-bentonite. ($C_m = 3 \text{ g L}^{-1}$; $r = 200 \text{ rpm}$; $\text{pH} = 7$; $V = 100 \text{ mL}$; $t = 60 \text{ min}$).

regression. The D–R parameters were calculated from the slope and intercept of the straight line obtained by the way and shown in Table 4.

As seen from Table 4, it can be concluded that the Langmuir model fitted experimental data better than the Freundlich and D–R models, with the $R^2 > 0.98$ at any temperature, indicating that almost monolayer adsorption took place on bentonite. The values of Q_m obtained from the Langmuir model adsorption increased with the rise of temperature, indicating that the adsorption was enhanced at higher temperature. In addition, the equilibrium adsorption capacity of Co

(II) was higher than the values reported in the literature [3].

As for the D–R model, the E values obtained from Table 4 were 17.27 (at $T = 298.15 \text{ K}$), 17.66 (at $T = 308.15 \text{ K}$), 18.47 (at $T = 318.15 \text{ K}$), and 18.73 kJ mol^{-1} (at $T = 328.15 \text{ K}$) for Co(II) ion, while 18.80 (at $T = 298.15 \text{ K}$), 20.64 (at $T = 308.15 \text{ K}$), 21.00 (at $T = 318.15 \text{ K}$), and 20.82 kJ mol^{-1} (at $T = 328.15 \text{ K}$) for Mn(II) ions, which were in the adsorption energy range of chemical ion-exchange reaction [21]. It is clear that Co(II) and Mn(II) ions adsorbed onto bentonite should be attributed to chemical adsorption rather

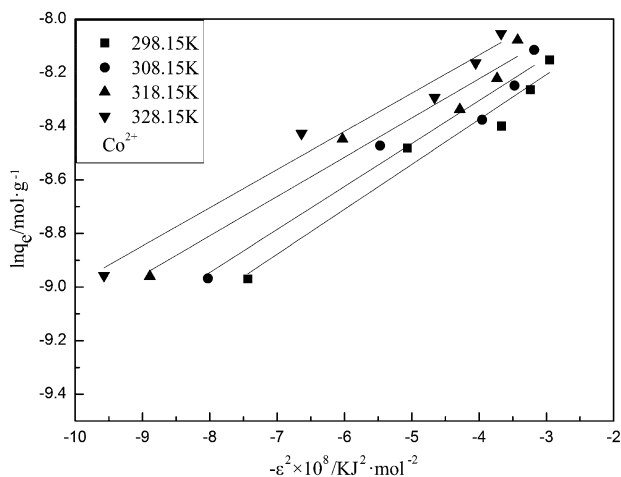


Fig. 9. D–R adsorption isotherm of Co(II) ion on Na-bentonite. ($C_m = 3 \text{ g L}^{-1}$; $r = 200 \text{ rpm}$; $\text{pH} = 7$; $V = 100 \text{ mL}$; $t = 60 \text{ min}$).

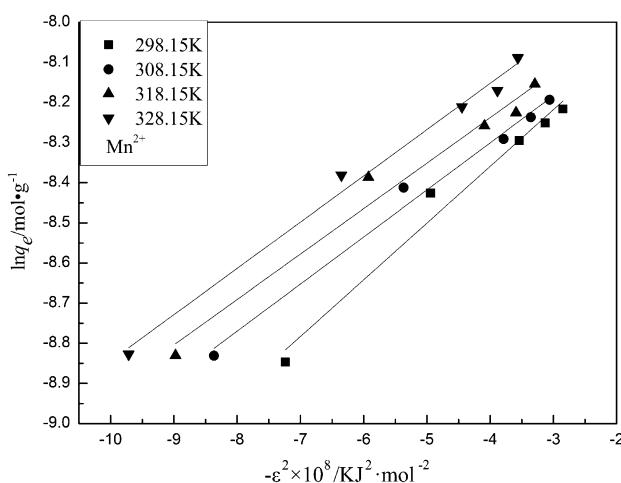


Fig. 10. D–R adsorption isotherm of Mn(II) ion on Na-bentonite. ($C_m = 3 \text{ g L}^{-1}$; $r = 200 \text{ rpm}$; $\text{pH} = 7$; $V = 100 \text{ mL}$; $t = 60 \text{ min}$).

than physical adsorption. The adsorption capacities, Q_m , derived from the D–R model were higher than those derived from the Langmuir model, which may be attributed to the different assumptions considered in the formulation of the isotherms [23].

3.7. Adsorption thermodynamic

The amounts of adsorption of Co(II) and Mn(II) metal ions by Na-bentonite were measured at 298.15, 308.15, 318.15, and 328.15 K, respectively. Thermodynamic parameters were calculated for this system using the following equations:

$$\ln K_D = \frac{\Delta S}{R} - \frac{\Delta H}{RT} \quad (13)$$

$$K_D = \frac{Q_e}{C_e} \quad (14)$$

where K_D is the distribution coefficient and T (K) is the temperature in kelvin, and R ($\text{J mol}^{-1} \text{K}^{-1}$) is the gas constant, respectively. The plots of $\ln K_D$ against $1/T$ for metal ions were shown in Fig. 11. The values of ΔH and ΔS were obtained from the slope and intercept of $\ln K_D$ vs. $1/T$ plots, which were calculated by a curve-fitting program. ΔG was computed using the well-known formula:

$$\Delta G = \Delta H - T\Delta S \quad (15)$$

The results were exhibited in Table 5.

The values of ΔH and ΔS were all positive, which suggested that the adsorption should be endothermic. The Gibbs free energy ΔG decreased with increasing temperature as shown in Table 5, indicating that the adsorption reaction was spontaneous and more favorable at higher temperature. The same type of behavior has been reported earlier [24,25].

The endothermic adsorption can be interpreted by the fact that the metal ions were well dissolved in water. They have to lose some part of their hydration sheath in terms of their adsorption onto Na-bentonite. This dehydration process of the metal ions requires energy and such energy supersedes the exothermicity

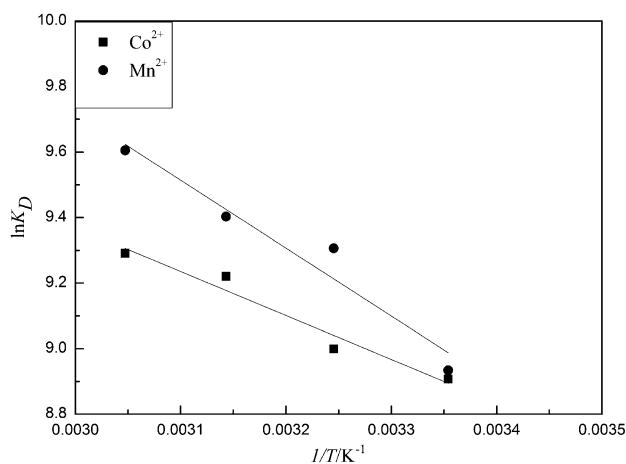


Fig. 11. Effect of temperature on the thermodynamic behavior of adsorption of metal ions on Na-bentonite ($C_{\text{Co}^{2+}} = 30 \text{ mg L}^{-1}$; $C_{\text{Mn}^{2+}} = 30 \text{ mg L}^{-1}$; $C_m = 3 \text{ g L}^{-1}$; $r = 200 \text{ rpm}$; $\text{pH} = 7$; $V = 100 \text{ mL}$; $t = 60 \text{ min}$).

Table 5

The values of the thermodynamic parameters for the adsorption of metal ions on Na-bentonite

Metal	ΔH (kJ mol ⁻¹)	ΔS (J mol ⁻¹ K ⁻¹)	ΔG (kJ mol ⁻¹)			
			298.15 K	308.15 K	318.15 K	328.15 K
Co ²⁺	11.1696	111.4076	-22.0466	-23.1606	-24.2747	-25.3888
Mn ²⁺	17.2422	132.5509	-22.2778	-23.6033	-24.9288	-26.2543

of the ions getting attach to the solid surface [24]. It may be inferred that both adsorption and ion exchange take place at low temperature, while only ion exchange occurs with increasing temperature [26]. The positive ΔS insinuated the adsorbability of the Na-bentonite toward metal ions in aqueous solutions and could account for some structure changes of the adsorbent. The metal complexes and the steric hindrance of adsorbed adsorbates form a resultant effect, which eventually result in the increase of the enthalpy and entropy [27].

3.8. Material characterization

In the PTA wastewater, the Co(II) and Mn(II) coexist, and the competitive adsorption does not happen in the adsorption process of Co(II) and Mn(II) onto the bentonite. Accordingly, SEM, XRD, and BET technologies were employed after both Co(II) and Mn(II) had been adsorbed onto the bentonite.

Fig. 12(a) and (b) are the SEM images of Na-bentonite and adsorbed Na-bentonite, respectively, and their surface morphologies are obviously different. Fig. 12 shows that the Na-bentonite superficial area is large and the lamellar structure stacked together tightly. The bentonite surface became loose and there occurs space between layers of bentonite. These results may be explained by two causes. One reason is that

the metal ions were adsorbed onto the surface and made the surface to be more porous and fluffy [28]. The other one is that the bentonite adsorbed some water because of its hydrophilicity, making the interlayer space enlarge [29].

The XRD patterns of Na-bentonite (A) and adsorbed bentonite (B) between the angles 10° and 90° are presented in Fig. 13. It is observed from this figure that the d_{001} peak is 0.9023 nm for Na-bentonite and 0.9446 nm for adsorbed bentonite, indicating the d-spacing is increased. Moreover, the XRD result of adsorbed bentonite showed that there was a decrease in the intensity and an increase in the width of the peaks [28]. The explanation is that the metal ions have intercalated between the layers and resulted in the change in bentonite structure.

Na-bentonite and adsorbed bentonite were also characterized with respect to specific surface area, total pore volume, and average pore diameter. The surface area, total pore volume, and pore size of Na-bentonite are 31.9875 m² g⁻¹, 0.0808 mL g⁻¹, and 10.102 nm, respectively. After adsorption of Co(II) and Mn(II) ions, these values become 37.9819 m² g⁻¹, 0.093 mL g⁻¹, and 9.7764 nm, respectively.

It is observed that the surface area and total pore volume of the bentonite were enlarged slightly after the adsorption of metal ions. Yet, the pore size diminished insignificantly. These results may be explained

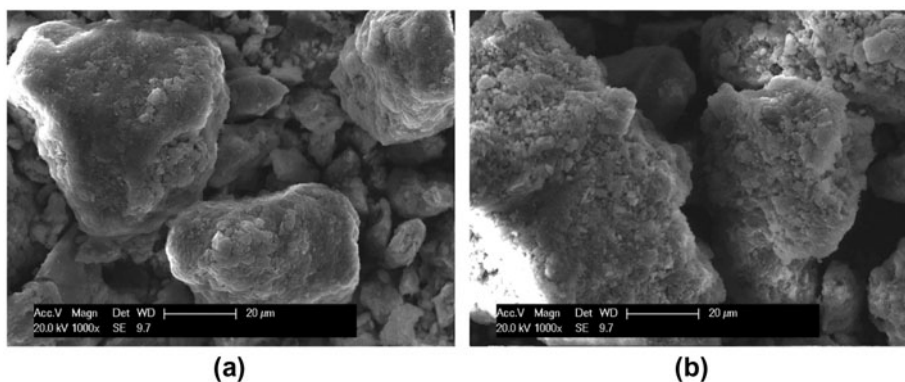


Fig. 12. SEM image (a) Na-bentonite and (b) adsorbed bentonite.

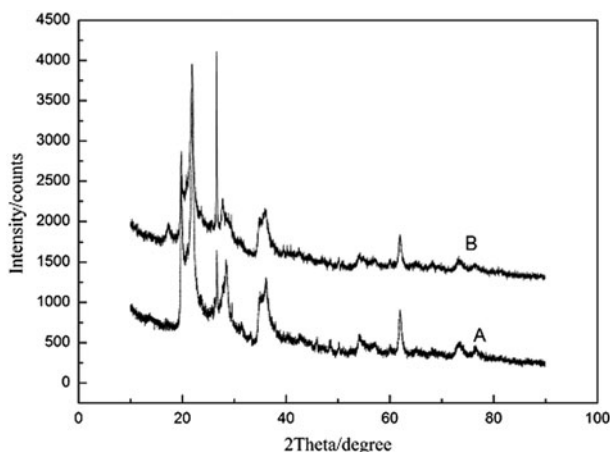


Fig. 13. The XRD patterns of (A) Na-bentonite and (B) adsorbed bentonite.

that the adsorbates generated some micropores when the heavy metal ions adsorbed onto the solid surface, which made the superficial area increase. In addition, Co(II) and Mn(II) ions inserted to the layers of bentonite or the micropores should result in increasing of the total pore volume and decreasing of the pore size [30]. The situations agreed with the SEM and XRD characterization well according to the analysis [31].

4. Conclusions

The results of this investigation suggested that the Na-bentonite should be an effective adsorbent for the removal of metal cations from PTA wastewater. Bentonite is readily available, cheap, and environment friendly, which make it a promising adsorbent used to deal with industrial effluents. The adsorption conditions, such as initial pH, temperature, and adsorbent dosage, should be designed precisely in practical work.

The Langmuir model agreed with experimental data better than the Freundlich and D–R models, demonstrating that the adsorption process is a monolayer adsorption. The values of Q_m obtained from the Langmuir model increased with the increasing temperature. The enthalpy changes, ΔH and ΔS , are all positive values, which suggest that the adsorption of metal ions onto Na-bentonite should be endothermic and spontaneous. The adsorption is more favorable at higher temperature because the value of ΔG decreases with increasing temperature.

The E values obtained from the D–R model are $17.27 \text{ kJ mol}^{-1}$ (at $T = 298.15 \text{ K}$) for Co(II) ion, while $E = 18.80 \text{ kJ mol}^{-1}$ (at $T = 298.15 \text{ K}$) for Mn(II) ion. Therefore, the adsorption of Co(II) and Mn Co(II) ions

onto Na-bentonite was a chemical adsorption rather than a physical adsorption. The main adsorption mechanism is ion exchange, and there may be some physical adsorption at all. The BET, SEM, and XRD analysis demonstrated that the Co(II) and Mn(II) ions were adsorbed onto the bentonite successfully, and the internal and external structures of the adsorbent have transformed more or less.

Acknowledgments

The authors would like to thank the National Natural Science Foundation of China (No. 21176049), Project of Fujian Province Department of Science & Technology (2014Y0066) and Nature Science Foundation of Fujian Province (No. 2012J01034).

References

- [1] G. Guan, W. Li, H. Wan, X. Qiao, J. Wang, A. Wu, The progress of technology of dealing with pure terephthalic acid wastewater, *Petrochem Technol.* 34 (2005) 715–719.
- [2] E.A. Sigworth, S.B. Smith, Adsorption of inorganic compounds by activated carbon, *Am. Water Works Assoc.* 64 (1972) 386–391.
- [3] Ş. Kubilay, R. Gürkan, A. Savran, T. Şahan, Removal of Cu(II), Zn(II) and Co(II) ions from aqueous solutions by adsorption onto natural bentonite, *Adsorption* 13 (2007) 41–51.
- [4] B. Gözen, Z.A. Ayse, Z.O. Mustafa, Removal of Pb(II), Cd(II), Cu(II), and Zn(II) from aqueous solutions by adsorption on bentonite, *J. Colloid Interface Sci.* 187 (1997) 338–343.
- [5] N.L. Dias Filho, Y. Gushikem, W.L. Polito, J.C. Moreira, E.O. Ehirim, Sorption and preconcentration of metal ions in ethanol solutions with silica gel modified with benzinimidazole, *Talanta* 42 (1995) 1625–1630.
- [6] U.M. Saha, K. Iwasaki, K. Sakurai, Desorption behavior of Cd, Zn and Pb sorbed on hydroxy aluminum and hydroxy aluminosilicate-montmorillonite complexes, *Clays Clay Miner.* 51(5) (2003) 481–492.
- [7] Y. Chen, W. Ye, X. Yang, F. Deng, Y. He, Effect of contact time, pH, and ionic strength on Cd(II) adsorption from aqueous solution onto bentonite from Gaomiaozi, China, *Environ. Earth Sci.* 64 (2011) 329–336.
- [8] A.S. Sheta, A.M. Falatah, M.S. Al-Sewailem, E.M. Khaled, A.S.H. Sallam, Sorption characteristics of zinc and iron by natural zeolite and bentonite, *Microporous Mesoporous Mater.* 61 (2003) 127–136.
- [9] R.A. García-delgado, Influence of soil carbonates in lead fixation, *J. Environ. Sci. Health Part A* 31 (1996) 2099–2109.
- [10] Y.S. Ho, Citation review of Lagergren kinetic rate equation on adsorption reaction, *Scientometrics* 59 (2004) 171–177.
- [11] M. Sarkar, A.R. Sarkar, J.L. Goswami, Mathematical modeling for the evaluation of zinc removal efficiency on clay sorbent, *J. Hazard. Mater.* 149 (2007) 666–674.

- [12] Y.S. Ho, G. McKay, A comparison of chemisorption kinetic models applied to pollutant removal on various sorbents, *Trans. Inst. Chem. Eng.* 76B (1998) 332–340.
- [13] F. Barbier, G. Duc, M. Petit-Ramel, Adsorption of lead and cadmium ions from aqueous solution to the montmorillonite/water interface, *Colloids Surf., A: Physicochem. Eng. Aspects* 166 (2000) 153–159.
- [14] S. Arfaoui, N. Frini-Srasra, E. Srasra, Modelling of the adsorption of the chromium ion by modified clays, *Desalination* 222 (2008) 474–481.
- [15] Q. Liu, T. Zheng, P. Wang, J. Jiang, N. Li, Adsorption isotherm, kinetic and mechanism studies of some substituted phenols on activated carbon fibers, *Chem. Eng. J.* 157 (2010) 348–356.
- [16] P. Senthil Kumar, S. Ramalingam, C. Senthamarai, M. Niranjanaa, P. Vijayalakshmi, S. Sivanesan, Adsorption of dye from aqueous solution by cashew nut shell: Studies on equilibrium isotherm, kinetics and thermodynamics of interactions, *Desalination* 261 (2010) 52–60.
- [17] H. Kalavathy, B. Karthik, L.R. Miranda, Removal and recovery of Ni and Zn from aqueous solution using activated carbon from *Hevea brasiliensis*: Batch and column studies, *Colloids Surf. B: Biointerfaces* 78 (2010) 291–302.
- [18] H. Chen, A. Wang, Kinetic and isothermal studies of lead ion adsorption onto palygorskite clay, *J. Colloid Interface Sci.* 307 (2007) 309–316.
- [19] X. Wang, Y. Zheng, A. Wang, Fast removal of copper ions from aqueous solution by chitosan-g-poly(acrylic acid)/attapulgitite composites, *J. Hazard. Mater.* 168 (2009) 970–977.
- [20] Z.G. Zhao, The application of Langmuir equation in the adsorption in dilute solution, *Univ. Chem.* 14(5) (1999) 7–10.
- [21] M.M. Saeed, Adsorption profile and thermodynamic parameters of the preconcentration of Eu(III) on 2-thenoyltrifluoroacetone loaded polyurethane(PRU) foam, *J. Radioanal. Nucl. Chem.* 256 (2003) 73–80.
- [22] M.A. Ahmad, N.K. Rahman, Equilibrium kinetics and thermodynamic of Remazol Brilliant Orange 3R dye adsorption on coffee husk-based activated carbon, *Chem. Eng. J.* 170 (2011) 154–161.
- [23] S. Yang, J. Li, Y. Lu, X. Wang, Sorption of Ni(II) on GMZ bentonite: Effects of pH, ionic strength, foreign ions, humic acid and temperature, *Appl. Radiat. Isot.* 67 (2009) 1600–1608.
- [24] R. Naseem, S.S. Tahir, Removal of Pb(II) from aqueous/acidic solutions by using bentonite as an adsorbent, *Water Res.* 35 (2001) 3982–3986.
- [25] S.S. Tahir, R. Naseem, Thermodynamics of Fe(II) and Mn(II) adsorption onto bentonite from aqueous solutions, *J. Chem. Thermodyn.* 32 (2000) 651–658.
- [26] S. Chegrouche, A. Mellah, S. Telmoune, Removal of lanthanum from aqueous solutions by natural bentonite, *Water Res.* 31 (1997) 1733–1737.
- [27] S.M. Hasany, M.M. Saeed, M. Ahmed, Separation of radionuclides by polyurethane foam, *J. Radioanal. Nucl. Chem.* 246 (2000) 581–587.
- [28] X. Yang, Z. Zhong, Y. Pan, X. Cheng, Adsorption characters and mechanisms of heavy metal ions in Na-bentonite, *Chin. J. Environ. Eng.* 7 (2013) 2775–2780.
- [29] D.M. Manohar, B.F. Noeline, T.S. Anirudhan, Adsorption performance of Al-pillared bentonite clay for the removal of cobalt(II) from aqueous phase, *Appl. Clay Sci.* 31 (2006) 194–206.
- [30] H. Zhang, Z. Tong, T. Wei, Y. Tang, Removal characteristics of Zn(II) from aqueous solution by alkaline Ca-bentonite, *Desalination*, 276(1–3) (2011) 103–108.
- [31] H. Zhang, Z. Tong, T. Wei, Y. Tang, Sorption characteristics of Pb(II) on alkaline Ca-bentonite, *Appl. Clay Sci.* 65–66 (2012) 21–23.